

STRUCTURE OF CHLORIC ACID HYDRATES AND EQUILIBRIUM COMPOSITION OF THE HClO₄-H₂O SYSTEM

V. D. Maiorov^{1*}, I. S. Kislina¹,
and E. G. Tarakanova^{2**}

Composition, structure, energy parameters, and existence regions of hydrate complexes formed in the HClO₄-H₂O system are studied by IR spectroscopy and quantum chemical methods. Three concentration-structural regions are determined. The HClO₄-H₂O solutions diluted to the 1:13.3 molar ratio of components contain ClO₄⁻ and H₅O₂⁺ solvate-separated ions, each hydrated by four water molecules. More concentrated solutions (1:13.3-1:5) contain hydrated ion pairs ClO₄⁻ · H₅O₂⁺ that are contact ion pairs if the [HClO₄]:[H₂O] ratio falls within the region 1:9-1:5. As the acid concentration increases further up to the transition of the HClO₄-H₂O system into the solid phase, pair complexes are formed. The structure of the latter is formed by a cycle of two contact ion pairs ClO₄⁻ · H₅O₂⁺ connected by two H-bonds. The solid phase consists of interacting polymer chains formed by ClO₄⁻ · H₅O₂⁺ and ClO₄⁻ · H₃O⁺ ion pairs.

DOI: 10.1134/S0022476624070059

Keywords: HClO₄ aqueous solution, hydrogen bond, hydrate structure, IR spectroscopy, quantum chemical calculations.

INTRODUCTION

In aqueous perchlorate solutions, ClO₄⁻ anions undergo negative hydration (according to the terminology by Samoilov [1]), i.e. water molecules in the anion's hydration shell form H-bonds with its oxygen atoms, and the bonds are weaker than those between water molecules in the pure solvent. The IR spectra of such solutions contain an intense band caused by vibrations of those OH bonds of water molecules that interact with anions. The maximum of the band is at ~3500 cm⁻¹ [2] (2630 cm⁻¹ in D₂O solutions [3]). According to the melting diagram [4], NaClO₄ aqueous solutions contain NaClO₄·6H₂O complexes in a wide range of component concentrations, while significant excess of water leads to complete dissociation of the salt into ions and formation of ClO₄⁻ tetrahydrate anions [2] and Na⁺ hexahydrate cations [5].

In our previous work (JSC, 2023, 112758), we established the equilibrium composition of the NaClO₄-H₂O system, determined the structure of NaClO₄·6H₂O complexes, and quantitatively explained changes in the IR spectra in the regions of bending and stretching vibrations of water molecules and the overtone at 6900 cm⁻¹. It was shown that only complexes with

¹Semenov Federal Research Center for Chemical Physics, Russian Academy of Sciences, Moscow, Russia; *vproton@bk.ru. ²Kurnakov Institute of General and Inorganic Chemistry, Russian Academy of Sciences, Moscow, Russia; **egtara@igic.ras.ru. Original article submitted December 25, 2023; revised February 28, 2024; accepted February 28, 2024.

the 1:6 composition can participate in some stages of acid catalyzed hydrolysis of esters by enhancing the nucleophilic assistance and thereby increasing the reaction rate [6, 7].

According to the melting diagram, the $\text{HClO}_4\text{-H}_2\text{O}$ system undergoes numerous structural changes manifested as a number of maxima corresponding to crystal hydrates with compositions 1:1 (49.9 °C), 1:2 (-20.65 °C), 1:2.5 (-32.1 °C), 1:3 (-40.2 °C), 1:3.5 (-45.6 °C), 1:4 (-58.0 °C), where digits in parentheses indicate melting points of the complexes [8]. The data reported in [8] were used in the calculations of the $\text{HClO}_4\text{-H}_2\text{O}$ system.

The IR spectra of the $\text{HClO}_4\text{-H}_2\text{O}$ system were analyzed and interpreted using a comprehensive experimental and computational approach based on the regularities characterizing the formation of hydrogen-bonded complexes in solutions [9]. This approach was earlier successfully utilized to study intercomponent interactions in various liquid acid-base systems [10-15]. According to these regularities, each molecular complex in the solutions is the most stable one in the series of isomers, has a cyclic or polycyclic structure, contains unstrained H-bonds, and has the most dense molecular packing among all complexes with similar compositions. As the solution concentration changes, the structure of each next complex is formed from the structure of the previous one with minimal energy costs and structural transformations. The solution with the highest content of complexes of the same type also contains a small number of complexes with previous and subsequent compositions.

The purpose of the present work is to determine the equilibrium composition of the $\text{HClO}_4\text{-H}_2\text{O}$ system and to establish the structure of the hydrate complexes formed in the system. To this aim, IR spectra of aqueous HClO_4 solutions were recorded and analyzed, and quantum chemical calculations of perchloric acid hydrates were conducted.

EXPERIMENTAL

In the experiments, perchloric acid (reagent-grade) was used. Aqueous HCl solutions were prepared by saturating distilled water with gaseous HCl. The concentration of initial aqueous HClO_4 and HCl solutions was determined by alkalimetric titration. Solutions with lower acid concentrations were prepared by weight dilution.

The IR spectra were recorded at 30 °C by the method of multiple frustrated total internal reflection (MFTIR) [16] on an attachment with a Ge working element providing a radiation incidence angle of 30°. The effective thickness of the absorbing layer at a frequency 2000 cm^{-1} was $3.35\text{ }\mu\text{m}$. The spectra were measured in the $1300\text{-}4000\text{ cm}^{-1}$ frequency range at the HClO_4 concentrations of $0\text{-}8.69\text{ mol/L}$ ($[\text{H}_2\text{O}]:[\text{HClO}_4] = 3.89$) and HCl concentrations of $0\text{-}11.65\text{ mol/L}$ ($[\text{H}_2\text{O}]:[\text{HCl}] = 3.59$). The band absorbances (D) were determined from the baselines with an accuracy of 5-7%. The optical density of continuous absorption was measured relative to the absorbance of the empty cuvette.

COMPUTATIONAL DETAILS

Total energies and optimal configurations of HClO_4 molecules, $\text{HClO}_4\cdot n\text{H}_2\text{O}$ ($n = 1\text{-}9$), $2\text{HClO}_4\cdot n\text{H}_2\text{O}$ ($n = 2\text{-}12$) hydrate complexes, and the polymer chain fragment $(\text{HClO}_4)_8\cdot(\text{H}_2\text{O})_8$ were calculated by the density functional theory method (B3LYP/6-31++G(d,p)) using the Gaussian09 program [17]. The structure of each $\text{HClO}_4\cdot n\text{H}_2\text{O}$ ($n = 1\text{-}9$) hydration complex was determined by considering all those possible relative arrangements of their molecules, which are compatible with the laws determining the formation of H-bonded complexes in solutions [9], and then choosing the most stable one. The paired complexes were calculated in the assumption that each of them is formed by two $\text{HClO}_4\cdot n\text{H}_2\text{O}$ complexes or by $\text{HClO}_4\cdot n\text{H}_2\text{O}$ and $\text{HClO}_4\cdot(n+1)\text{H}_2\text{O}$ complexes. The analysis of stationary points on the potential energy surfaces of the studied systems showed that their optimal configurations correspond to energy minima (all elements of the Hessian matrices are positive).

When estimating formation energies (ΔE) of hydrate complexes and polymer chain fragment, their total electronic energies were used under the assumption that a negligibly small restructuring energy is required for a molecule as it is incorporated into an H-bonded complex of any composition and structure. Therefore, the formation energy of each hydrate

was calculated by subtracting the energies of its molecules from the total hydrate energy. Similarly, when estimating the formation energy of the $2\text{HClO}_4 \cdot n\text{H}_2\text{O}$ paired complex (ΔE_p) from two complexes, each containing one HClO_4 molecule, their total energies were subtracted from that of the paired complex.

Hydrogen bonds in the figures with optimized geometries of the complexes and fragments of the polymer structure satisfy the following conditions: bond lengths $< 3 \text{ \AA}$, and their number and directions correspond to those of the lone pairs of oxygen atoms.

RESULTS AND DISCUSSION

Computation results. According to the melting diagram, complexes with stoichiometric compositions 1:2.5 and 1:3.5 are formed in the $\text{HClO}_4\text{-H}_2\text{O}$ system [8]. We assumed that these are stable paired complexes obtained due to the combination of complexes $\text{HClO}_4 \cdot n\text{H}_2\text{O}$ and $\text{HClO}_4 \cdot (n+1)\text{H}_2\text{O}$ ($n = 2, 3$). Complexes with close compositions are similarly formed due to the combination of two complexes $\text{HClO}_4 \cdot n\text{H}_2\text{O}$ ($n = 2-4$). This assumption is supported by the fact that the transition from the largest of these paired complexes ($2\text{HClO}_4 \cdot 8\text{H}_2\text{O}$) to the $\text{HClO}_4 \cdot 5\text{H}_2\text{O}$ complex, containing one HClO_4 molecule, proceeds through minimal structural changes and energy costs, in full agreement with the laws discussed in [9, 10, 12-15]. The fact that the $\text{HClO}_4\text{-H}_2\text{O}$ system (in contrast to most of the earlier studied systems containing one paired complex with the composition 2:2 [9, 12-15]) has a range of concentrations where various paired complexes are formed may be explained by the presence of four H-bond forming oxygen atoms in the HClO_4 molecule.

The equilibrium composition of the $\text{HClO}_4\text{-H}_2\text{O}$ system was determined by calculating two series of H-bonded complexes, $\text{HClO}_4 \cdot n\text{H}_2\text{O}$ ($n = 1-9$) and $2\text{HClO}_4 \cdot n\text{H}_2\text{O}$ ($n = 2-12$), while structural and energetic parameters of polymer chains in the solid phase were studied by calculating the $8\text{HClO}_4 \cdot 8\text{H}_2\text{O}$ fragment. Table 1 lists total energies (E) and formation energies (ΔE) of these complexes, as well as the formation energy (ΔE_p) for each of the studied paired complexes composed of two complexes, each containing one HClO_4 molecule.

Fig. 1 and 2 show optimized geometries of the studied hydrates. The first figure shows three complexes with a 1:1 stoichiometric ratio of molecules and complexes containing one molecule of the $\text{HClO}_4 \cdot n\text{H}_2\text{O}$ acid ($n = 2-9$); the second figure shows paired complexes, except for the $2\text{HClO}_4 \cdot 2\text{H}_2\text{O}$ heterotetramer.

Structural and energy parameters of complexes $\text{HClO}_4 \cdot n\text{H}_2\text{O}$ ($n = 1-9$). As a result of optimization, the proton of the HClO_4 molecule in the $\text{HClO}_4 \cdot n\text{H}_2\text{O}$ complexes with $n > 2$ passed on to the H_2O molecule, thus forming three conjugated hydrogen bridges inside the complex (Fig. 1e-k). Parameters of two such bridges are identical in the $\text{HClO}_4 \cdot 3\text{H}_2\text{O}$ hydrate and differ for all three bridges in other complexes (Table 2). Note that the length of the shortest and least asymmetric hydrogen bridge ($r(\text{O} \cdots \text{O}) = 2.487\text{-}2.560 \text{ \AA}$) is in all cases characteristic for the H_5O_2^+ ion whose structure is distorted under the influence of surrounding species. Therefore, it can be stated that complexes $\text{HClO}_4 \cdot n\text{H}_2\text{O}$ ($n = 3-9$) contain ClO_4^- anions and H_5O_2^+ cations. (Despite this structural transformation, the optimized ion-containing complexes we will be referred to below as $n\text{HClO}_4 \cdot m\text{H}_2\text{O}$).

Note that the ClO_4^- anion and the H_5O_2^+ ion in $\text{HClO}_4 \cdot n\text{H}_2\text{O}$ complexes ($n = 3-9$) interact with each other via one or two H-bonds, thus forming a contact ion pair (Fig. 1e-k). Even though the relative arrangement of the counterions and the interaction between them can vary in different complexes, this ionic pair is the basis of the hydrate structure. Therefore, the solvate-separated ion pairs are formed and the $\text{HClO}_4 \cdot n\text{H}_2\text{O}$ complexes are separated into hydrated H_5O_2^+ and ClO_4^- at a smaller than 1:9 molar ratio of the $\text{HClO}_4\text{-H}_2\text{O}$ solution components.

The calculation results indicate that H_5O_2^+ and ClO_4^- tend to participate in the interactions between the species in varying degrees. In the $\text{HClO}_4 \cdot n\text{H}_2\text{O}$ ($n \geq 4$) hydrates, the H_5O_2^+ ion forms four H-bonds, using all its capabilities. At the same time, the ClO_4^- anion has three free lone pairs even for $n = 9$. The anion forms only three H-bonds in small

TABLE 1. Total Energies (E , hartree) and Formation Energies (ΔE , kcal/mol) of $\text{HClO}_4 \cdot n\text{H}_2\text{O}$ and $m\text{HClO}_4 \cdot n\text{H}_2\text{O}$ Hydrate Complexes; Formation Energies of $2\text{HClO}_4 \cdot n\text{H}_2\text{O}$ Complexes Composed of Two Complexes Containing One HClO_4 Molecule (E_p , kcal/mol)

Complex	$-E$	ΔE	ΔE_p	Figure number (in the present work)
$\text{HClO}_4 \cdot \text{H}_2\text{O}$	837.770489	12.33	–	1a
$2\text{HClO}_4 \cdot 2\text{H}_2\text{O}$	1675.557921	35.30	10.63	1b
$8\text{HClO}_4 \cdot 8\text{H}_2\text{O}$	6702.307366	188.68	–	1c
$\text{HClO}_4 \cdot 2\text{H}_2\text{O}$	914.225113	25.18	–	1d
$\text{HClO}_4 \cdot 3\text{H}_2\text{O}$	990.680732	38.67	–	1e
$\text{HClO}_4 \cdot 4\text{H}_2\text{O}$	1067.135373	51.53	–	1f
$\text{HClO}_4 \cdot 5\text{H}_2\text{O}$	1143.590785	64.92	–	1g
$\text{HClO}_4 \cdot 6\text{H}_2\text{O}$	1220.045874	78.08	–	1h
$\text{HClO}_4 \cdot 7\text{H}_2\text{O}$	1296.503540	92.85	–	1i
$\text{HClO}_4 \cdot 8\text{H}_2\text{O}$	1372.956280	104.53	–	1j
$\text{HClO}_4 \cdot 9\text{H}_2\text{O}$	1449.408551	115.92	–	1k
$2\text{HClO}_4 \cdot 3\text{H}_2\text{O}$	1752.015839	50.23	12.70	2a
$2\text{HClO}_4 \cdot 4\text{H}_2\text{O}$	1828.476692	67.00	16.61	2b
$2\text{HClO}_4 \cdot 5\text{H}_2\text{O}$	1904.930582	79.41	15.52	2c
$2\text{HClO}_4 \cdot 6\text{H}_2\text{O}$	1981.391478	96.21	18.83	2d
$2\text{HClO}_4 \cdot 7\text{H}_2\text{O}$	2057.843710	107.57	17.32	2e
$2\text{HClO}_4 \cdot 8\text{H}_2\text{O}$	2134.299280	121.03	17.91	2f
$2\text{HClO}_4 \cdot 9\text{H}_2\text{O}$	2210.748057	130.22	13.74	2g
$2\text{HClO}_4 \cdot 10\text{H}_2\text{O}$	2287.199555	141.13	11.29	2h
$2\text{HClO}_4 \cdot 11\text{H}_2\text{O}$	2363.654746	154.35	11.37	2i
$2\text{HClO}_4 \cdot 12\text{H}_2\text{O}$	2440.110794	168.10	11.91	2j

$\text{HClO}_4 \cdot n\text{H}_2\text{O}$ complexes ($n = 3$ and 4) and four in larger complexes ($n = 5-8$), while one of its oxygen atoms never participates in the interactions between the species. In the largest calculated hydrate containing one acid molecule ($\text{HClO}_4 \cdot 9\text{H}_2\text{O}$), the ClO_4^- anion forms five H-bonds (using all four oxygen atoms), while H_2O molecules are interconnected by six H-bonds. They strongly interact with each other also in other cases (Fig. 1*h-j*). Thus, in the series of $\text{HClO}_4 \cdot n\text{H}_2\text{O}$ complexes containing the H_5O_2^+ ion, it is energetically most favorable for water molecules to form H-bonds with this ion, while the interaction with other water molecules rather than with the ClO_4^- anion is more profitable in the case of its complete hydration. This result agrees with the fact that ClO_4^- anions exhibit negative hydration in perchlorate aqueous solutions [1, 2].

Structural and energy parameters of $2\text{HClO}_4 \cdot n\text{H}_2\text{O}$ complexes ($n = 2-12$). The $2\text{HClO}_4 \cdot 2\text{H}_2\text{O}$ complex with alternating acid and water molecules (Fig. 1*b*) contains two hydrogen bridges, in each of which the proton of the HClO_4 molecule approaches the oxygen of the H_2O molecule without passing to it (Table 2). The energy required for this complex to form two $\text{HClO}_4 \cdot \text{H}_2\text{O}$ complexes (Fig. 1*a*) is 10.63 kcal/mol (Table 1). The structure of $2\text{HClO}_4 \cdot 2\text{H}_2\text{O}$ complexes allows them to be H-bonded into infinite polymer chains interacting with each other, which is a condition for a solution to transform into the solid phase [18]. Fig. 1*c* shows the optimized geometry of the chain fragment composed of four $2\text{HClO}_4 \cdot 2\text{H}_2\text{O}$ complexes. As can be seen, protons of HClO_4 molecules (except those at the ends of the fragment) in the $8\text{HClO}_4 \cdot 8\text{H}_2\text{O}$ fragment move to H_2O molecules to form $\text{ClO}_4^- \cdot \text{H}_3\text{O}^+$ ion pairs. This result agrees with a high melting point of perchloric acid monohydrate [8].

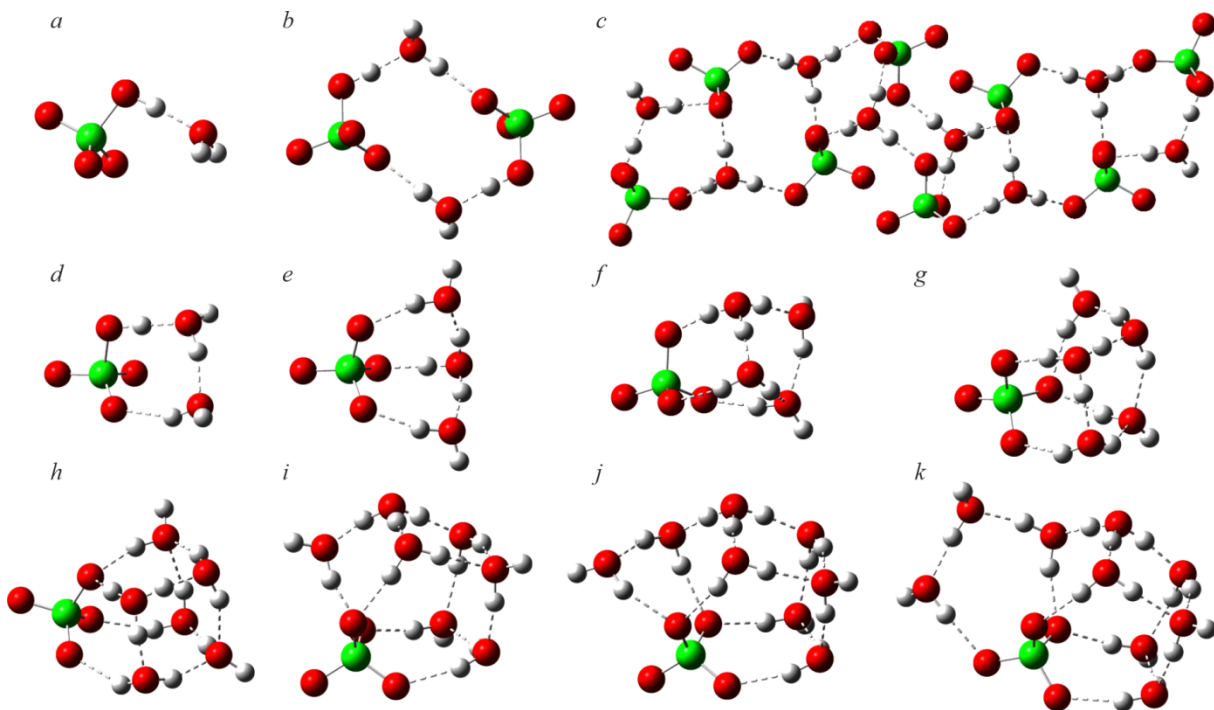


Fig. 1. Structure of hydrate complexes $\text{HClO}_4 \cdot \text{H}_2\text{O}$ (a), $2\text{HClO}_4 \cdot 2\text{H}_2\text{O}$ (b), $8\text{HClO}_4 \cdot 8\text{H}_2\text{O}$ (c), $\text{HClO}_4 \cdot 2\text{H}_2\text{O}$ (d), $\text{HClO}_4 \cdot 3\text{H}_2\text{O}$ (e), $\text{HClO}_4 \cdot 4\text{H}_2\text{O}$ (f), $\text{HClO}_4 \cdot 5\text{H}_2\text{O}$ (g), $\text{HClO}_4 \cdot 6\text{H}_2\text{O}$ (h), $\text{HClO}_4 \cdot 7\text{H}_2\text{O}$ (i), $\text{HClO}_4 \cdot 8\text{H}_2\text{O}$ (j), and $\text{HClO}_4 \cdot 9\text{H}_2\text{O}$ (k). In figures *f-k*, the H_5O_2^+ ion is at the top.

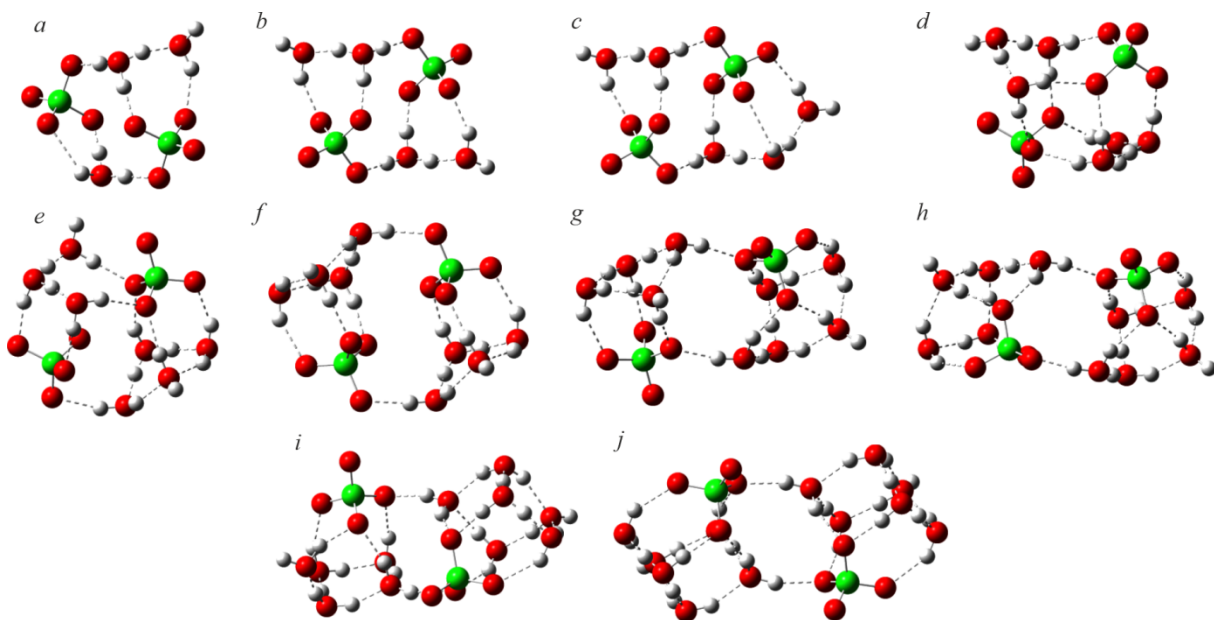


Fig. 2. Structure of hydrate complexes $2\text{HClO}_4 \cdot 3\text{H}_2\text{O}$ (a), $2\text{HClO}_4 \cdot 4\text{H}_2\text{O}$ (b), $2\text{HClO}_4 \cdot 5\text{H}_2\text{O}$ (c), $2\text{HClO}_4 \cdot 6\text{H}_2\text{O}$ (d), $2\text{HClO}_4 \cdot 7\text{H}_2\text{O}$ (e), $2\text{HClO}_4 \cdot 8\text{H}_2\text{O}$ (f), $2\text{HClO}_4 \cdot 9\text{H}_2\text{O}$ (g), $2\text{HClO}_4 \cdot 10\text{H}_2\text{O}$ (h), $2\text{HClO}_4 \cdot 11\text{H}_2\text{O}$ (i), and $2\text{HClO}_4 \cdot 12\text{H}_2\text{O}$ (j).

As the content of water in the $\text{HClO}_4\text{--H}_2\text{O}$ system increases, $2\text{HClO}_4 \cdot 4\text{H}_2\text{O}$ complexes are formed after $2\text{HClO}_4 \cdot 2\text{H}_2\text{O}$ complexes (within the polymer chains) (Fig. 2*b*). Each of them consists of two $\text{HClO}_4 \cdot 2\text{H}_2\text{O}$ complexes, which combined together so that the protons of their HClO_4 molecules passed to the H_2O molecules. As a result, two ClO_4^- anions

TABLE 2. Interatomic Distances in the Bridge of the H_5O_2^+ Ion and in the Conjugated Hydrogen Bridges of Complexes $\text{HClO}_4 \cdot n\text{H}_2\text{O}$ ($n = 3-9$) and $2\text{HClO}_4 \cdot n\text{H}_2\text{O}$ ($n = 3-12$)

Complex	Bridge of the H_5O_2^+ ion			Conjugated bridge I			Conjugated bridge II		
	$r(\text{O} \cdots \text{H})$	$r(\text{H} \cdots \text{O})$	$r(\text{O} \cdots \text{O})$	$r(\text{O} \cdots \text{H})$	$r(\text{H} \cdots \text{O})$	$r(\text{O} \cdots \text{O})$	$r(\text{O} \cdots \text{H})$	$r(\text{H} \cdots \text{O})$	$r(\text{O} \cdots \text{O})$
$\text{HClO}_4 \cdot 3\text{H}_2\text{O}$	1.033	1.527	2.560	1.026	1.541	2.567	1.026	1.541	2.567
$\text{HClO}_4 \cdot 4\text{H}_2\text{O}$	1.046	1.494	2.540	1.024	1.558	2.582	1.019	1.573	2.592
$\text{HClO}_4 \cdot 5\text{H}_2\text{O}$	1.072	1.418	2.490	1.033	1.536	2.569	0.992	1.732	2.724
$\text{HClO}_4 \cdot 6\text{H}_2\text{O}$	1.053	1.467	2.520	1.044	1.498	2.542	1.003	1.687	2.690
$\text{HClO}_4 \cdot 7\text{H}_2\text{O}$	1.054	1.458	2.512	1.036	1.519	2.555	1.016	1.568	2.584
$\text{HClO}_4 \cdot 8\text{H}_2\text{O}$	1.047	1.473	2.520	1.034	1.521	2.555	1.025	1.558	2.583
$\text{HClO}_4 \cdot 9\text{H}_2\text{O}$	1.062	1.425	2.487	1.030	1.537	2.567	1.022	1.572	2.594
$2\text{HClO}_4 \cdot 3\text{H}_2\text{O}$	1.030	1.511	2.541	1.022	1.545	2.567	1.009	1.615	2.624
$2\text{HClO}_4 \cdot 4\text{H}_2\text{O}$	1.031	1.512	2.543	1.020	1.555	2.575	1.012	1.603	2.615
$2\text{HClO}_4 \cdot 5\text{H}_2\text{O}$	1.033	1.505	2.538	1.015	1.589	2.604	1.015	1.591	2.606
	1.076	1.401	2.477	1.007	1.624	2.631	1.000	1.677	2.677
$2\text{HClO}_4 \cdot 6\text{H}_2\text{O}$	1.089	1.365	2.454	1.003	1.634	2.637	1.003	1.643	2.646
	1.062	1.435	2.497	1.027	1.517	2.544	0.999	1.681	2.680
$2\text{HClO}_4 \cdot 7\text{H}_2\text{O}$	1.061	1.448	2.509	1.033	1.505	2.538	0.997	1.745	2.742
	1.069	1.419	2.488	1.039	1.508	2.547	0.985	1.901	2.886
$2\text{HClO}_4 \cdot 8\text{H}_2\text{O}$	1.070	1.413	2.483	1.032	1.540	2.572	0.995	1.733	2.728
$2\text{HClO}_4 \cdot 9\text{H}_2\text{O}$	1.065	1.425	2.490	1.034	1.533	2.567	1.000	1.684	2.684
	1.085	1.388	2.473	1.044	1.482	2.526	0.990	1.795	2.785
$2\text{HClO}_4 \cdot 10\text{H}_2\text{O}$	1.085	1.388	2.473	1.045	1.475	2.520	0.992	1.770	2.762
$2\text{HClO}_4 \cdot 11\text{H}_2\text{O}$	1.106	1.351	2.457	1.010	1.605	2.615	1.005	1.670	2.675
$2\text{HClO}_4 \cdot 12\text{H}_2\text{O}$	1.062	1.446	2.508	1.049	1.477	2.526	0.994	1.751	2.745

and two H_5O_2^+ cations (the structure of the latter is distorted compared to that in the gas phase) were formed inside $2\text{HClO}_4 \cdot 4\text{H}_2\text{O}$. At the same time, the bridge of each H_5O_2^+ ion is connected with two unstrained hydrogen bridges (Table 2). The structure of the $2\text{HClO}_4 \cdot 4\text{H}_2\text{O}$ complex can be described as a cycle composed of two $\text{H}_5\text{O}_2^+ \cdot \text{ClO}_4^-$ contact ion pairs connected by two H-bonds. Each ion pair also has a cyclic structure where the cation and the anion are connected by two H-bonds.

The structure of $2\text{HClO}_4 \cdot 4\text{H}_2\text{O}$ complexes allows them to combine with each other and with $2\text{HClO}_4 \cdot 2\text{H}_2\text{O}$ complexes into infinite interconnected polymer chains. For the molar component ratio 1:1.5, in the case of equal amounts of $2\text{HClO}_4 \cdot 2\text{H}_2\text{O}$ complexes (in the form of $\text{H}_3\text{O}^+ \cdot \text{ClO}_4^-$ ion pairs) and $2\text{HClO}_4 \cdot 4\text{H}_2\text{O}$ complexes, the system exists in the solid state ($T_m = 26^\circ\text{C}$) [8]. As the fraction of $2\text{HClO}_4 \cdot 4\text{H}_2\text{O}$ complexes increases (with increasing water concentration), the melting temperature decreases and the system transforms into the liquid phase [8], apparently because H_5O_2^+ ions form weaker H-bonds with the environment than H_3O^+ ions. Structural features of $2\text{HClO}_4 \cdot 4\text{H}_2\text{O}$ complexes suggest that they interact with each other in solutions to form small polymer chains.

Adding one water molecule to the $2\text{HClO}_4 \cdot 4\text{H}_2\text{O}$ complex followed by the formation of the $2\text{HClO}_4 \cdot 5\text{H}_2\text{O}$ complex (Fig. 2c) does not significantly affect the structure of this compound (the framework of the $2\text{HClO}_4 \cdot 4\text{H}_2\text{O}$ complex is maintained). A characteristic feature of the resulting compound is that it is formed at the boundary between two concentration-structural regions. The first of them contains complexes consisting of two contact ion pairs, and the second one contains hydrated contact ion pairs.

The next complex, $2\text{HClO}_4 \cdot 6\text{H}_2\text{O}$ (Fig. 2d), consists of two $\text{HClO}_4 \cdot 3\text{H}_2\text{O}$ complexes that were strongly deformed during the optimization. The complexes are connected by four H-bonds whose total energy (18.83 kcal/mol) exceeds the ΔE_p values of other paired complexes (Table 1). Two of these bonds connect the contact ion pairs to each other; each of the other two H-bonds is formed by a water molecule hydrating two contact ion pairs.

The $2\text{HClO}_4 \cdot n\text{H}_2\text{O}$ complexes ($n = 7-12$) contain hydrated contact ion pairs with counterions sharing a common hydrogen bond (Fig. 2e-k). Components of the $2\text{HClO}_4 \cdot 7\text{H}_2\text{O}$ complex ($\text{HClO}_4 \cdot 3\text{H}_2\text{O}$ and $\text{HClO}_4 \cdot 4\text{H}_2\text{O}$) are connected by four H-bonds (Fig. 2e). In the complexes $2\text{HClO}_4 \cdot n\text{H}_2\text{O}$ ($n = 7-8$), similarly to the paired ones with a lower water content ($n = 3-6$), two contact ion pairs are connected by two H-bonds. In larger complexes ($n = 9-12$), the interaction between ion pairs is much weaker (Table 1). The $2\text{HClO}_4 \cdot 9\text{H}_2\text{O}$ complex contains one H-bond, and two contact ion pairs are separated by water molecules beginning from $2\text{HClO}_4 \cdot 10\text{H}_2\text{O}$. Weakening the interaction between the individual parts of paired complexes will lead to their dissociation in the solution and subsequent formation of complexes containing one HClO_4 molecule (Fig. 1g-k).

The above results explain why paired complexes are formed in the $\text{HClO}_4\text{-H}_2\text{O}$ system at the molar component ratio $\geq 1:4$, while $\text{HClO}_4 \cdot n\text{H}_2\text{O}$ complexes are formed in more dilute solutions ($n = 5-9$). The structure of $2\text{HClO}_4 \cdot n\text{H}_2\text{O}$ ($n = 4-8$) complexes is based on a very strong cycle composed of two $\text{ClO}_4^- \cdot \text{H}_5\text{O}_2^+$ contact ion pairs connected by two H-bonds. Therefore, in contrast to the complexes with weakly interacting constituent parts $2\text{HClO}_4 \cdot n\text{H}_2\text{O}$ ($n \geq 9$), such complexes do not break down in the solution into smaller complexes containing one HClO_4 molecule.

Our calculations indicate that the $\text{HClO}_4\text{-H}_2\text{O}$ system contains the following concentration-structural regions. Components of the most concentrated solutions are partially or completely connected into $2\text{HClO}_4 \cdot 4\text{H}_2\text{O}$ cyclic complexes composed of two $\text{H}_5\text{O}_2^+ \cdot \text{ClO}_4^-$ contact ion pairs. For lower acid contents, the following paired complexes are formed in solutions: $2\text{HClO}_4 \cdot 5\text{H}_2\text{O}$, $2\text{HClO}_4 \cdot 6\text{H}_2\text{O}$, $2\text{HClO}_4 \cdot 7\text{H}_2\text{O}$, and $2\text{HClO}_4 \cdot 8\text{H}_2\text{O}$. The complexes contain hydrated ion pairs where counterions are still bonded to each other. Even more dilute solutions ($[\text{HClO}_4]:[\text{H}_2\text{O}]$ from 1:5 to 1:9) contain complexes comprising one acid molecule each and also consisting of $\text{ClO}_4^- \cdot \text{H}_5\text{O}_2^+ \cdot n\text{H}_2\text{O}$ hydrated contact ion pairs ($n = 5-9$).

Thus, there is the following explanation of the melting curve structure [8]. As the solution temperature decreases, paired complexes combined into interacting chain structures characterized by relatively high melting points [8].

Asymmetry degree of $\text{O} \cdots \text{H} \cdots \text{O}$ hydrogen bridges as a function of their length. Another interesting result was obtained by analysing the parameters of three conjugated hydrogen bridges in the $2\text{HClO}_4 \cdot n\text{H}_2\text{O}$ ($n = 4-8$) and $\text{HClO}_4 \cdot n\text{H}_2\text{O}$ ($n = 5-9$) complexes observed in the studied solutions. It was established for $r(\text{O} \cdots \text{O}) < 2.6 \text{ \AA}$ that there is a linear dependence between the length of the $\text{O} \cdots \text{H} \cdots \text{O}$ bridge and its asymmetry degree (Fig. 3) characterized by the coefficient K_{asym} equal to the ratio between long and short H-bonds of the bridge ($r(\text{H} \cdots \text{O})/r(\text{O} \cdots \text{H})$). Linear nature of this dependence in the considered range of $r(\text{O} \cdots \text{O})$ values indicates that two main structural parameters ($r(\text{O} \cdots \text{O})$ and K_{asym}) in short hydrogen bridges (e.g. in H_5O_2^+ ions) change symbatically with the molecular environment. The deviation of this dependence from a straight line increases with increasing distance between the oxygen atoms. Using these data, the proton position in the H_5O_2^+ ion bridge can be estimated only from its $r(\text{O} \cdots \text{O})$ length.

IR spectroscopy study. Fig. 4 shows MFTIR spectra of water and aqueous perchloric acid solution with a concentration of 6.6 mol/L (39.8 mol/L H_2O). The differences observed in these spectra over the entire frequency range are due to the formation of H_5O_2^+ hydrated ions with strong quasi-symmetric H-bonds in $\text{O} \cdots \text{H} \cdots \text{O}$ bridges [19-21] and due to the hydration of ClO_4^- anions. A characteristic feature of the IR spectra of H_5O_2^+ ions is continuous absorption (CA) in the region from 900 cm^{-1} to 4000 cm^{-1} caused by the presence of a large number of overlapping intense high-order bands arising due to the electro-optical anharmonicity of the $\text{O} \cdots \text{H} \cdots \text{O}$ bridge and strong kinematic interaction between its coordinates and the ligand coordinates [22]. The spectrum of H_5O_2^+ ions exhibit a number of separate bands on the background of continuous absorption [23].

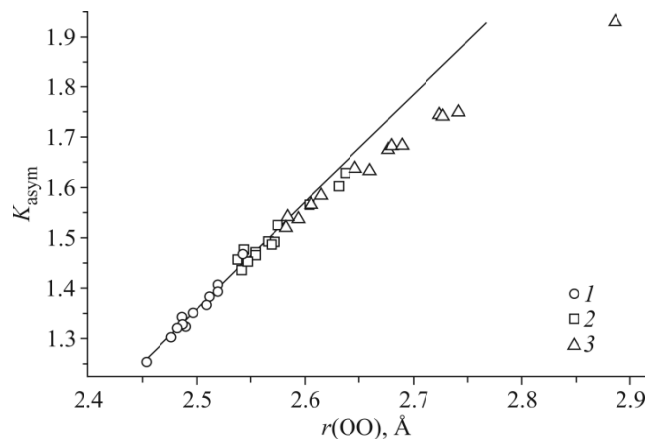


Fig. 3. Asymmetry coefficient of conjugated hydrogen bridges in $2\text{HClO}_4 \cdot n\text{H}_2\text{O}$ ($n = 4-8$) and $\text{HClO}_4 \cdot n\text{H}_2\text{O}$ ($n = 5-9$) complexes as a function of their length. Designations: asymmetry coefficients (K_{asym}) of the H_5O_2^+ bridge (1), first (2), and second (3) conjugated bridges.

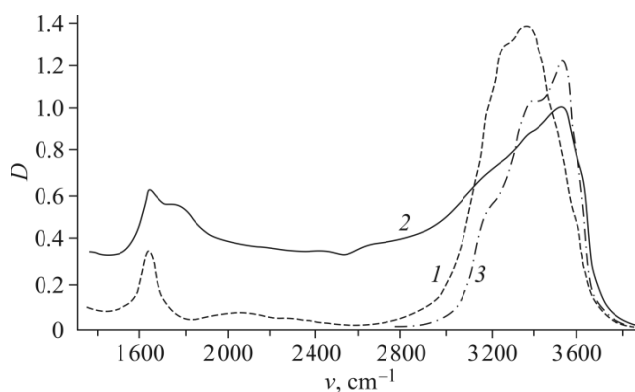


Fig. 4. MFTIR spectra of water (1), aqueous perchloric acid solution (6.6 mol/L HClO_4 , 39.8 mol/L H_2O) (2) and sodium perchlorate solution (7.3 mol/L NaClO_4 , 35.5 mol/L H_2O) (3). The thickness of the absorption layer is 3.35 μm .

The changes in the IR spectra of aqueous NaClO_4 solutions due to the ion hydration are localized near the band maxima at 1640 cm^{-1} and 3500 cm^{-1} (JSC, 2023, 112758), Fig. 4, spectrum 3. To establish characteristics of ClO_4^- hydration in aqueous HClO_4 solutions, contributions of the H_5O_2^+ absorption spectrum to the total absorbance in these regions should be determined. This was done as follows.

In addition to the contribution from water molecules, the D_{3500} IR spectra of aqueous HClO_4 solutions have also a contribution of H_5O_2^+ ions. The value of the latter was determined from the IR spectroscopy data obtained for aqueous HCl solutions. The spectral characteristic of H_5O_2^+ ions is continuous absorption that does not depend (according to the mechanism of its formation) on the HA acid anion [22, 24]. We will prove it on the example of HClO_4 and HCl aqueous solutions (Fig. 5) for which CA absorbances and acid concentrations were compared at a frequency of 2000 cm^{-1} . The contribution of water molecules should be also considered since they exhibit some weak absorption at this frequency. Therefore, the D_{2000}^* absorbance caused only by the absorption of H_5O_2^+ ions was searched by subtracting the contribution of water molecules not involved in the formation of these ions from the experimental D_{2000} values:

$$D_{2000}^* = D_{2000} - \varepsilon_{2000}(\text{H}_2\text{O}) \cdot l_{2000} \cdot ([\text{H}_2\text{O}]_0 - 2[\text{HA}]_0) = \varepsilon_{2000}(\text{H}_5\text{O}_2^+) \cdot l_{2000} \cdot [\text{HA}]_0, \quad (1)$$

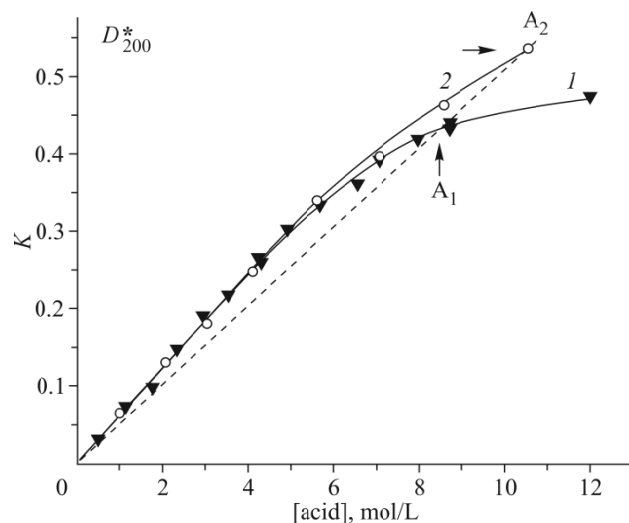


Fig. 5. D_{2000}^* as a function of HClO_4 (1) and HCl (2) concentration. Symbols A_1 and A_2 denote acid concentrations in HClO_4 and HCl aqueous solutions with equal water:acid ratios equal to 4.09.

where $\varepsilon_{2000}(\text{H}_2\text{O})$, $\varepsilon_{2000}(\text{H}_5\text{O}_2^+)$ are absorption coefficients for water and H_5O_2^+ ions; l_{2000} is the effective absorption layer thickness at a frequency of 2000 cm^{-1} .

In relatively dilute solutions of both acids, the D_{2000}^* values exhibit the same dependence: CA absorbance grows linearly up to the values 4.9 mol/L HClO_4 and 5.6 mol/L HCl , corresponding for such HClO_4 and HCl concentrations to equal component ratios $[\text{HA}]_0:[\text{H}_2\text{O}]_0 = 1:8.8$. The $\varepsilon_{2000}(\text{H}_5\text{O}_2^+)$ absorption coefficients for both acids are equal to $180\text{ L}/(\text{mol}\cdot\text{cm})$. In more concentrated solutions, the linearity is violated, the $\varepsilon_{2000}(\text{H}_5\text{O}_2^+)$ coefficients decrease, and dependences demonstrated by HClO_4 and HCl solutions diverge (Fig. 5). This discrepancy is not due to the anion influence on $\varepsilon_{2000}(\text{H}_5\text{O}_2^+)$ and corresponds to the $[\text{HA}]_0:[\text{H}_2\text{O}]_0$ ratios that depend differently on the concentrations of HClO_4 and HCl acids. We will show that the $\varepsilon_{2000}(\text{H}_5\text{O}_2^+)$ values coincide at the same component ratios in HClO_4 and HCl solutions. Fig. 5 shows compositions of HClO_4 (A_1) and HCl (A_2) solutions with equal component ratios ($[\text{HA}]_0:[\text{H}_2\text{O}]_0 = 4.1$). The dashed line starts from the coordinate origin and passes through both of these points, and its inclination angle determines the $\varepsilon_{2000}(\text{H}_5\text{O}_2^+)$ coefficient value at the given component ratio. The following analysis of IR spectra of aqueous HClO_4 solutions was performed under the assumption that the IR spectrum of H_5O_2^+ ions is not affected by the anions.

The contributions to the D_{3500} absorbance in aqueous HClO_4 solutions with a significant excess of water include the absorption of H_5O_2^+ ions, water molecules, hydrating ClO_4^- anions, and water molecules not involved in the hydration of anions and the formation of H_5O_2^+ ions.

$$D_{3500} = \varepsilon_{3500}(\text{H}_5\text{O}_2^+)l_{3500} \cdot [\text{HClO}_4]_0 + 4\varepsilon_{\text{hydr}}l_{3500} \cdot [\text{HClO}_4]_0 + \varepsilon l_{3500} \cdot ([\text{H}_2\text{O}]_0 - 6[\text{HClO}_4]_0). \quad (2)$$

Equation (2) takes into account that the acid is completely dissociated, the anion is hydrated by four water molecules, and two more water molecules are required to form the H_5O_2^+ ion. Here, $\varepsilon_{3500}(\text{H}_5\text{O}_2^+)$, $\varepsilon_{\text{hydr}}$, and ε are absorption coefficients of H_5O_2^+ ions, water molecules hydrating the anions, and water molecules not involved in the anion hydration and the formation of H_5O_2^+ ions, respectively; l_{3500} is the effective absorbing layer thickness at 3500 cm^{-1} . For aqueous HCl solutions, (2) is written as follows:

$$D_{3500} = \varepsilon_{3500}(\text{H}_5\text{O}_2^+)l_{3500} \cdot [\text{HCl}]_0 + \varepsilon l_{3500} \cdot ([\text{H}_2\text{O}]_0 - 2[\text{HCl}]_0)$$

and

$$D_{3500} / ([\text{H}_2\text{O}]_0 - 2[\text{HCl}]_0) = \varepsilon l_{3500} + \varepsilon_{3500}(\text{H}_5\text{O}_2^+)l_{3500} \cdot [\text{HCl}]_0 / ([\text{H}_2\text{O}]_0 - 2[\text{HCl}]_0). \quad (3)$$

The linear correlation (3) is true throughout the considered concentration range from 0 to 10.6 ($[\text{HCl}]_0:[\text{H}_2\text{O}]_0 = 1:4.1$) mol/L HCl, $\varepsilon_{3500}(\text{H}_5\text{O}_2^+)l_{3500} = 0.017$ L/mol (Fig. 6). Note that the difference $([\text{H}_2\text{O}]_0 - 2[\text{HCl}]_0)$ in (3) includes two kinds of water molecules: those which do and do not participate in H_5O_2^+ hydration. Therefore, the obtained linear correlation (3) indicates that the spectral manifestations of these water molecules in the region of OH stretchings are identical.

The $\varepsilon_{3500}(\text{H}_5\text{O}_2^+)l_{3500}$ coefficient value equal to 0.017 L/mol was used to determine the contribution of H_5O_2^+ absorption to the absorbance at 3500 cm^{-1} in HClO_4 aqueous solutions. This way, we calculated D_{3500}^* values equal to $D_{3500} - \varepsilon_{3500}(\text{H}_5\text{O}_2^+)l_{3500}[\text{HClO}_4]_0$, and obtained (4) from (2) for the subsequent experimental data analysis:

$$D_{3500}^* / ([\text{H}_2\text{O}]_0 - 6[\text{HClO}_4]_0) = \varepsilon l_{3500} + \varepsilon_{\text{hydr}}l_{3500} \cdot 4[\text{HClO}_4]_0 / ([\text{H}_2\text{O}]_0 - 6[\text{HClO}_4]_0). \quad (4)$$

The $\varepsilon_{\text{hydr}}l_{3500}$ value calculated from the linear correlation in the coordinates of equation (4) (Fig. 7) is equal to 0.017 L/mol and exceeds the εl_{3500} value for water molecules in a pure solvent by ~35%. This is significantly less than in NaClO_4 aqueous solutions where $\varepsilon_{\text{hydr}}$ exceeds ε more than doubly (JSC, 2023, 112758). This difference is explained as follows. According to the quantum chemical calculations, the lengths of H-bonds between water molecules and oxygen atoms of the ClO_4^- ion vary much stronger for the complexes formed in the $\text{HClO}_4\text{-H}_2\text{O}$ system than in the $\text{NaClO}_4\text{-H}_2\text{O}$ system. This should correspond to a noticeable broadening of the 3500 cm^{-1} band in the spectra of acid solutions and to the decrease of the coefficient at its maximum, as was indeed observed in the experiment (Fig. 4). The linear dependence in Fig. 7 is observed in the HClO_4 concentration range from 0 to 5.2 mol/L ($[\text{HClO}_4]_0/([\text{H}_2\text{O}]_0) = 1:8.3$). The obtained data do not allow separating this range into individual concentration-structural regions with pronounced features of ClO_4^- hydration in HClO_4 aqueous solutions with a varying water excess.

We consider changes in the IR spectra of HClO_4 aqueous solutions in the region of water molecule bendings. The band at 1640 cm^{-1} overlaps with a band of scissoring vibrations of terminal groups of H_5O_2^+ ions with a maximum at 1720 cm^{-1} [25, 26]. Since the band is symmetrical [26], the H_5O_2^+ absorption is the same at 1800 cm^{-1} and 1640 cm^{-1} . Using

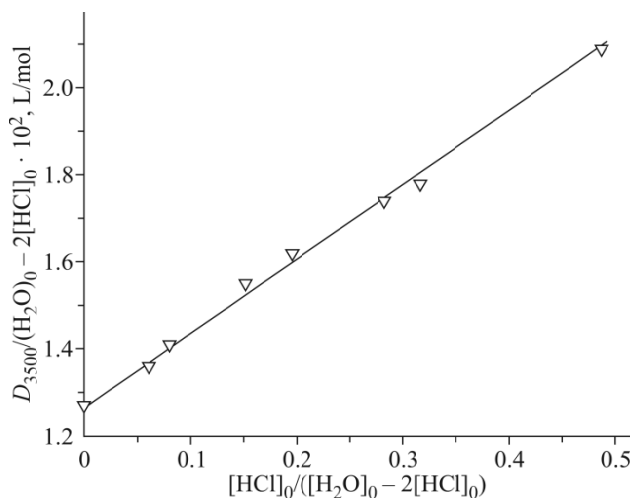


Fig. 6. Linear correlation in the coordinates of (3) at 3500 cm^{-1} in HCl aqueous solutions.

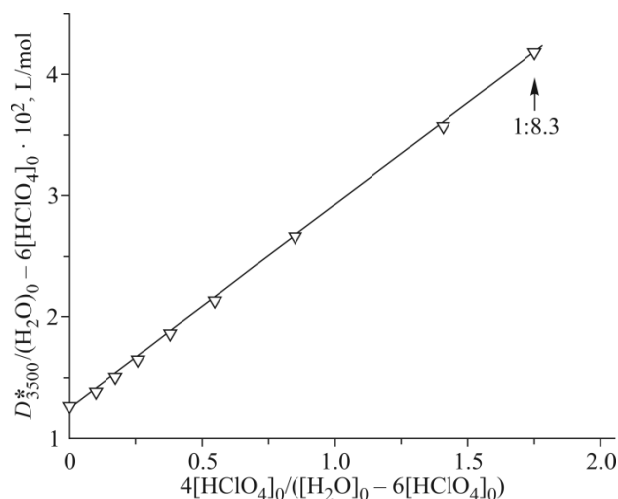


Fig. 7. Linear correlation in the coordinates of (4) at 3500 cm^{-1} in HClO_4 aqueous solutions.

this fact, we obtained D_{1640}^* values corresponding to the bendings of those water molecules that do not participate in the formation of H_5O_2^+ ions ($[\text{H}_2\text{O}]$ is the concentration of such molecules):

$$D_{1640}^* = D_{1640} - D_{1800},$$

$$[\text{H}_2\text{O}] = [\text{H}_2\text{O}]_0 - 2[\text{HClO}_4]_0.$$

It was earlier established that the absorption coefficients of water molecules that do and do not participate in the ClO_4^- hydration in dilute NaClO_4 aqueous solutions are equal at 1640 cm^{-1} . This is true up to the 1:11 component ratio (JSC 2023, 112758). Fig. 8 shows the dependence of D_{1640}^* on $[\text{H}_2\text{O}]$ for the $\text{HClO}_4\text{-H}_2\text{O}$ system: it is proportional in the 0-3.5 mol/L HClO_4 concentration range approximately up to $[\text{HClO}_4]_0:[\text{H}_2\text{O}]_0 = 1:13.3$. More concentrated solutions exhibit smaller absorption coefficients, and this range can be divided into two intervals. The absorption coefficient decreases insignificantly by no more than 10% up to the 1:6 molar component ratio and a decreases abruptly in more concentrated solutions so that its value for the 1:3.9 ratio is approximately 2.5 times lower than in dilute solutions.

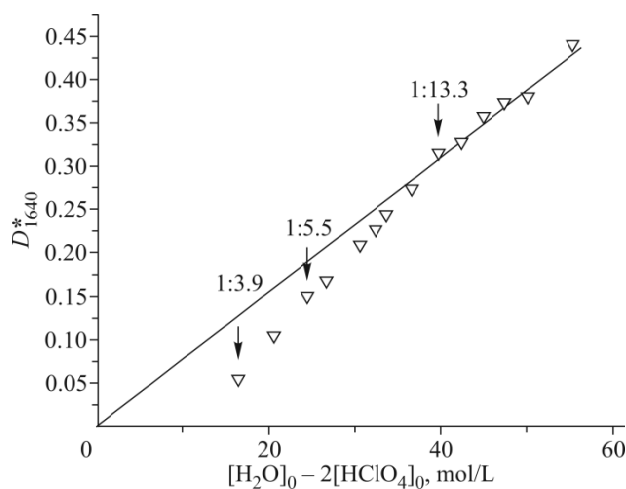


Fig. 8. D_{1640}^* as a function of $[\text{H}_2\text{O}]_0 - 2[\text{HClO}_4]_0$.

The obtained data indicate that the system $\text{HClO}_4\text{-H}_2\text{O}$ contains three concentration-structural regions. The first of them is a region of dilute solutions up to $[\text{HClO}_4]_0:[\text{H}_2\text{O}]_0 \approx 1:13.3$ containing solvate-separated ClO_4^- and H_5O_2^+ hydrated ions. The acid concentration ranges corresponding to this concentration-structural region obtained in our studies (up to 1:13.3) virtually coincide with the NMR data (up to 1:14) reported in [27, 28]). At a significant excess of water in HClO_4 solutions, two water molecules are involved in the formation of the H_5O_2^+ ion, and four water molecules participate in the formation of each solvation shell of the counterions.

The linear dependence of D_{1640}^* on $[\text{H}_2\text{O}]$ is violated (Fig. 8), apparently due to the fact that some water molecules are coordinated both with the anion and with the cation, thus forming ion pairs in the solutions. The calculation data suggest that the coefficient slightly decreases in solutions containing hydrated contact ion pairs with one HClO_4 molecule (second concentration-structural region) (Fig. 1g-k) and changes significantly due to the formation of paired complexes (third concentration-structural region) (Fig. 2b-f).

CONCLUSIONS

We conducted a comprehensive computational and experimental study of the composition, structure, energy parameters, and existence regions of hydrate complexes formed in the $\text{HClO}_4\text{-H}_2\text{O}$ system. The following concentration-structural regions were determined by comparing the calculation and IR spectroscopy data. Dilute solutions up to the 1:13.3 molar component ratio contain solvate-separated ClO_4^- and H_5O_2^+ hydrated ions. More concentrated solutions (1:13.3-1:5) contain hydrated solvate-separated or contact ion pairs, counterions of the latter being interconnected by one or two H-bonds. Below the 1:5 ratio, complexes containing two acid molecules are formed. Their structure is based on strong cycles composed of two contact ion pairs connected by two H-bonds. Such cyclic complexes with the general formula $2\text{ClO}_4^- \cdot 2\text{H}_5\text{O}_2^+ \cdot n\text{H}_2\text{O}$ ($n = 4-0$) are successively formed over a wide range of HClO_4 concentrations, and non-hydrated ion pairs ($n = 0$) are also formed after the $\text{HClO}_4\text{-H}_2\text{O}$ system transforms into the solid phase.

It was shown that short hydrogen bridges $\text{O}\cdots\text{H}\cdots\text{O}$ ($r(\text{O}\cdots\text{O}) < 2.6 \text{ \AA}$), in particular H_5O_2^+ ion bridges, exhibit a linear dependence between their length and the asymmetry degree. This fact can be used to estimate the proton position in the H_5O_2^+ ion bridge when only its length is known.

FUNDING

The IR spectra of solutions were measured, analyzed, and quantitatively interpreted using quantum chemical calculations within the Program of Fundamental Research of the Russian Federation (No. 122040500068-0).

The DFT study of structural and energy parameters of the hydrate complexes formed in $\text{HClO}_4\text{-H}_2\text{O}$ solutions and some interpretations of experimental data based on the calculation results were funded by the Ministry of Science and Higher Education of the Russian Federation as part of the State Assignment for Kurnakov Institute of General and Inorganic Chemistry of the Russian Academy of Sciences.

CONFLICT OF INTERESTS

The authors of this work declare that they have no conflicts of interest.

REFERENCES

1. O. Y. Samoilov. *Struktura vodnykh rastvorov elektrolitov i gidratatsiya ionov* (Structure of Aqueous Electrolyte Solutions and Ion Hydration). Moscow, Russia: Izd. Akad. Nauk SSSR, 1957. [In Russian]

2. A. G. Davidian. Stroyeniye vodnykh rastvorov perkhloratov metallov I-III grupp Periodicheskoi sistemy D.I. Mendeleeva (Structure of Aqueous Solutions of Metal Perchlorates of Groups I-III of the Periodic Table of D.I. Mendeleev): Cand. (Chem.) Dissertation. Peterhof, St. Petersburg, Russia: St. Petersburg State University, **2014**. [In Russian]
3. G. Brink and M. Falk. Infrared spectrum of HDO in aqueous solutions of perchlorates and tetrafluoroborates. *Can. J. Chem.*, **1970**, 48(19), 3019-3025. <https://doi.org/10.1139/v70-509>
4. A. N. Kirgintsev, L. N. Trushnikova, and V. G. Lavrent'eva. Rastvorimost' neorganicheskikh veshchestv v vode (Solubility of Inorganic Substances in Water). Leningrad, Russia: Khimiya, **1972**. [In Russian]
5. P. R. Smirnov and V. N. Trostin. Structure of the nearest surrounding of the Na⁺ ion in aqueous solutions of its salts. *Russ. J. Gen. Chem.*, **2007**, 77(5), 844-850. <https://doi.org/10.1134/s1070363207050052>
6. M. I. Vinnik. Some elementary reactions of acid-base processes in the liquid phase. *Bull. Acad. Sci. USSR, Div. Chem. Sci.*, **1973**, 22(5), 963-969. <https://doi.org/10.1007/bf00854232>
7. N. B. Librovich and M. I. Vinnik. Hydrolysis of formic acid esters in aqueous solutions of strong acids. *Russ. J. Phys. Chem. A*, **1979**, 53(12), 2993.
8. V. Y. Rosolovsky. Khimiya bezvodnoi khlornoj kisloty (Chemistry of Anhydrous Perchloric Acid). Moscow, Russia: Nauka, **1966**. [In Russian]
9. E. G. Tarakanova, G. V. Yukhnevich, I. S. Kislina, and V. D. Maiorov. Structure and regularities of formation of H-bonded complexes in aqueous and nonaqueous binary solutions. *Phys. Wave Phenom.*, **2020**, 28(2), 168-175. <https://doi.org/10.3103/s1541308x2002017x>
10. V. D. Maiorov, I. S. Kislina, and E. G. Tarakanova. Structure of complexes in the H₂SO₄-2-pyrrolidone system as determined by IR-spectroscopy and quantum-chemical calculations. *Russ. J. Phys. Chem. B*, **2017**, 11(1), 37-48. <https://doi.org/10.1134/s1990793117010080>
11. V. D. Maiorov, G. I. Voloshenko, and I. S. Kislina. Composition and structure of complexes formed in aqueous solutions of trifluoroacetic acid according to IR spectroscopy data. *Russ. J. Phys. Chem. B*, **2018**, 12(2), 185-191. <https://doi.org/10.1134/s1990793118020197>
12. E. G. Tarakanova and G. V. Yukhnevich. Structure of molecular complexes formed in aqueous solutions of trifluoroacetic acid. *J. Struct. Chem.*, **2014**, 55(8), 1409-1418. <https://doi.org/10.1134/s0022476614080058>
13. V. D. Maiorov, G. I. Voloshenko, I. S. Kislina, and E. G. Tarakanova. Composition and structure of hydrates formed in aqueous dimethylacetamide solutions. *Russ. J. Phys. Chem. B*, **2020**, 14(1), 5-14. <https://doi.org/10.1134/s199079312001008x>
14. E. G. Tarakanova, G. I. Voloshenko, I. S. Kislina, V. D. Mayorov, G. V. Yukhnevich, and A. K. Lyashchenko. Composition and structure of hydrates formed in aqueous solutions of formic acid. *J. Struct. Chem.*, **2019**, 60(2), 255-267. <https://doi.org/10.1134/s0022476619020100>
15. E. G. Tarakanova and G. V. Yukhnevich. Composition and structure of hydrates of CH₃COOH molecules and CH₃CO²⁻ anions in aqueous solutions. *J. Struct. Chem.*, **2017**, 58(7), 1357-1367. <https://doi.org/10.1134/s0022476617070125>
16. N. J. Harrick. Internal Reflection Spectroscopy. New York, Russia: Wiley Intersci., **1967**.
17. M. J. Frisch, G. W. Trucks, H. B. Schlegel, G. E. Scuseria, M. A. Robb, J. R. Cheeseman, G. Scalmani, V. Barone, B. Mennucci, G. A. Petersson, H. Nakatsuji, M. Caricato, X. Li, H. P. Hratchian, A. F. Izmaylov, J. Bloino, G. Zheng, J. L. Sonnenberg, M. Hada, M. Ehara, K. Toyota, R. Fukuda, J. Hasegawa, M. Ishida, T. Nakajima, Y. Honda, O. Kitao, H. Nakai, T. Vreven, J. A. Montgomery, J. E. Peralta, F. Ogliaro, M. Bearpark, J. J. Heyd, E. Brothers, K. N. Kudin, V. N. Staroverov, R. Kobayashi, J. Normand, K. Raghavachari, A. Rendell, J. C. Burant, S. S. Iyengar, J. Tomasi, M. Cossi, N. Rega, J. M. Millam, M. Klene, J. E. Knox, J. B. Cross, V. Bakken, C. Adamo, J. Jaramillo, R. Gomperts, R. E. Stratmann, O. Yazyev, A. J. Austin, R. Cammi, C. Pomelli, J. W. Ochterski, R. L. Martin, K. Morokuma, V. G. Zakrzewski, G. A. Voth, P. Salvador, J. J. Dannenberg, S. Dapprich, A. D. Daniels, O. Farkas, J. B. Foresman, J. V. Ortiz, J. Cioslowski, and D. J. Fox. Gaussian09, Revision A.02. Wallingford, CT, USA: Gaussian, Inc., **2009**.

18. E. G. Tarakanova and I. A. Kirilenko. Glass formation mechanism in aqueous formic acid solutions. *J. Non. Cryst. Solids*, **2021**, 573, 121130. <https://doi.org/10.1016/j.jnoncrysol.2021.121130>
19. M. V. Vener and N. B. Librovich. The structure and vibrational spectra of proton hydrates: as a simplest stable ion. *Int. Rev. Phys. Chem.*, **2009**, 28(3), 407-434. <https://doi.org/10.1080/01442350903079955>
20. R. Janoschek, A. Hayd, E. G. Weidemann, and M. Leuchs, G. Zundel. Calculated and observed isotope effects with easily polarizable hydrogen and deuterium bonds. *J. Chem. Soc., Faraday Trans. 2*, **1978**, 74, 1238. <https://doi.org/10.1039/f29787401238>
21. A. A. Pankov, V. Yu. Borovkov, and V. B. Kazanskii. IK-spektroskopicheskoe issledovanie perenosa protona v kompleksakh spirtov s galogengidridami v aprotonnykh rastvoritelyakh (IR spectroscopic study of the proton-transfer in complexes of alcohols with halogen hydrides in aprotic-solvents). *Dokl. Akad. Nauk SSSR*, **1981**, 258(4), 902. [In Russian]
22. G. V. Yukhnevich, E. G. Tarakanova, V. D. Mayorov, and N. B. Librovich. Nature of continuous absorption in IR spectra of charged complexes with a symmetric hydrogen bond. *J. Mol. Struct.*, **1992**, 265(3/4), 237-267. [https://doi.org/10.1016/0022-2860\(92\)80105-q](https://doi.org/10.1016/0022-2860(92)80105-q)
23. V. D. Maiorov and N. B. Librovich. IR spectrum of the H_5O_2^+ ion in acid solution. *Bull. Acad. Sci. USSR, Div. Chem. Sci.*, **1989**, 38(4), 872/873. <https://doi.org/10.1007/bf00953313>
24. N. B. Librovich, A. P. Devjatin, I. S. Kislina, V. D. Maiorov, and M. I. Vinnik. Issledovanie nepreryvnogo pogloshcheniya v infrakrasnom spektre sistemy $\text{HClO}_4\text{-NaClO}_4\text{-H}_2\text{O}$ (Investigation of continuous absorption in the infrared spectrum of the $\text{HClO}_4\text{-NaClO}_4\text{-H}_2\text{O}$ system). *Zh. Fiz. Khim.*, **1983**, 57(1), 200. [In Russian]
25. A. I. Karelin and Z. K. Nikitina. Infrared spectroscopic estimation of H^+ and D^+ positions in the structure of the orthorhombic crystals of $\text{H}_5\text{O}_2^+\text{ClO}_4^-$ and $\text{D}_5\text{O}_2^+\text{ClO}_4^-$. *J. Struct. Chem.*, **2015**, 56(2), 221-232. <https://doi.org/10.1134/s0022476615020043>
26. V. D. Maiorov, N. B. Librovich, and M. I. Vinnik. An investigation of proton solvation in aqueous sulfuric acid solutions based on the 1700 cm^{-1} absorption band in their IR spectra. *Bull. Acad. Sci. USSR, Div. Chem. Sci.*, **1979**, 28(2), 257-260. <https://doi.org/10.1007/bf00925861>
27. G. V. Lagodzinskaya, I. Y. Kozyreva, N. G. Yunda, and G. B. Manelis. Precision measurements of PMR chemical shifts in a strong magnetic field and structure of aqueous solutions of perchloric acid. *Bull. Acad. Sci. USSR, Div. Chem. Sci.*, **1984**, 33(10), 2017-2023. <https://doi.org/10.1007/bf00954073>
28. G. V. Lagodzinskaya, N. G. Yunda, and G. B. Manelis. Labile supramolecular structures and their dynamics in associated liquids based on NMR data. *Russ. Chem. Bull.*, **2006**, 55(4), 597-623. <https://doi.org/10.1007/s11172-006-0302-3>

Publisher's Note. Pleiades Publishing remains neutral with regard to jurisdictional claims in published maps and institutional affiliations.